GEOPHYSICS, VOL. 72, NO. 2 (MARCH-APRIL 2007); P. F85–F95, 12 FIGS., 1 TABLE.
10.1190/1.2437105

Electromagnetic imaging of a complex ore body: 3D forward modeling, sensitivity tests, and down-mine measurements

Pilar Queralt[1], Alan G. Jones[2], and Juanjo Ledo[1]

ABSTRACT

This study investigated the capability of audio-magnetotellurics (AMT) not only to detect, but also to delineate complex conductive ore bodies at minable depths. A detailed 3D numerical-electrical resistivity model of the Bathurst no. 12 deposit (New Brunswick, Canada) was constructed using available geologic and geophysical information. Different geologic and data acquisition conditions were simulated: presence of overburden; different geometries, dimensions, and positions of the ore body; and different data sampling regimes. The behavior of the surface 3D electromagnetic fields was compared with that from bodies of infinite strike extent. The 3D and 2D AMT responses were similar at high frequencies, so 2D modeling was shown to be both valid and sufficient. However, at low frequencies only those responses for current flow perpendicular to the body (the transverse magnetic mode in a 2D case), were reasonably similar. The 2D inversions showed that the position and the top of the 3D ore body were well resolved, but the bottom of the ore body's resistivity were poorly resolved. To increase resolution at depth below ore bodies, and to possibly extend mine life, we recommend that AMT measurements are taken from within mines. Simple mod-els of ore bodies were simulated to show responses at depth, and to undertake body stripping of the overlying structures. The tests showed that conductive structures above the measurement level can have a strong influence on imaging of conducting zones below, and can produce distortion effects in apparent resistivity and phase. Although the body-stripping approach reduces these effects and gives an indication of whether there are conductive structures below, the resulting image is considerably different from that of a model without overlying conductive structures. Full 3D inversion, holding known structures at constant, is required.

INTRODUCTION

Geophysical methods, particularly electromagnetic methods, have been very successfully used to discover economic base metal and precious metal ore bodies (e.g., Tripp, 2005). A common view is that all mineral deposits within 500 m of the surface, and close to existing infrastructure, have essentially been discovered and exploited, and are rapidly being depleted. Because of the high cost of installing new infrastructure in greenfield areas, the modern challenge is to determine if there are deeper deposits at economically recoverable depths (typically 1.5 to 2 km) within or close to existing deposits and infrastructure (e.g., Zhang et al., 1998; White and Gordon, 2003).

Controlled-source electromagnetic (CSEM) methods are superior to natural-source EM methods for probing shallow depths (e.g., Boerner et al., 1993), because the source is controllable and the survey can be designed for the problem at hand (e.g., Stummer et al., 2004). For deeper investigations (typically greater than about 500 m depth), natural-source EM methods, principally magnetotellurics (MT), offer distinct advantages over CSEM. These relate mainly to cost and logistic difficulties of the requirement for CSEM of two powerful, independently oriented bipole sources sufficiently distant from the recording locations that the target is not in the near field of the source (e.g., Boerner et al., 1993; Wannamaker, 1997). Additional advantages of MT over CSEM are superior data processing (remote-reference robust approaches, e.g., Jones et al., 1989; Egbert, 1997), distortion analyses (e.g., McNeice and Jones, 2001; Caldwell et al., 2004), and multidimensional modeling capabilities. In particular, the mathematical formulations for multidimensional modeling are more tractable in MT, and yield practical, efficient, and fast 2D

Manuscript received by the Editor March 3, 2006; revised manuscript received October 4, 2006; published online March 2, 2007.
[1]Departament de Geodinàmica i Geofísica, Universitat de Barcelona, Barcelona, Spain. Email: pilar.queralt@ub.edu; jledo@ub.edu.
[2]Dublin Institute for Advanced Studies, Dublin, Ireland. Email: alan@cp.dias.ie.

inversion and 3D forward inversion codes (e.g., 2D: Smith and Booker, 1991; Rodi and Mackie, 2001; 3D: Mackie et al., 1994; Siripunvaraporn et al., 2005). Over the last decade, these factors have proved MT to be a reliable method of EM imaging (Garcia and Jones, 2001), particularly when coupled with modern 24-bit acquisition systems, and continuous-profiling systems such as Mount Isa Mines' MIMDAS (Sheard, 2001) or Quantec's TITAN-24 (White and Gordon, 2003). As a direct consequence of these advances, the application of audio-MT (AMT) (i.e., MT at frequencies of 10 Hz to 10 kHz) for mineral exploration has increased significantly over the last decade, particularly for base and precious metals in Canada where it has been used at more than 25,000 sites, principally in Voisey's Bay, the Sudbury Basin, and the Thompson Nickel Belt (e.g., Balch et al., 1998; Stevens and McNeice, 1998; Zhang et al., 1998; Watts and Balch, 2000; Jones and Garcia, 2003).

The aim of our research was to study the capability of AMT not only to detect, but also to delineate complex conductive ore bodies at minable depths. Previous model-based studies have been undertaken in the Sudbury Basin (e.g., Livelybrooks et al., 1996); however, further work is required to achieve a better understanding of the applicability of AMT for mine-scale problems. Moreover, as an extension to surface-based methods, we advocate the use of EM data acquired from the lowest levels in mines, to detect ore that might exist below existing workings and thereby possibly extend mine life.

Three-dimensional modeling is essential to define the complex geometry of ore bodies, but reliable 3D inversion algorithms that can be applied to observed data are still in their infancy. Since the late 1970s, when 3D modeling was first developed, studies have been published on 3D effects in MT data (e.g., Wannamaker et al., 1980, 1984a, b; Ting and Hohmann, 1981; Jones, 1983) and recent studies have shown the main limitations of 2D inversion of 3D data (e.g., Garcia et al., 1999; Ledo et al., 2002; Ledo, 2005); these studies made recommendations to avoid 3D effects in 1D or 2D interpretations. Some 3D MT inversion codes are publicly available (e.g., Siripunvaraporn et al., 2005), but they are not in common use and, as was the case with 2D codes, it will be some time before they are developed into useful, reliable, and well-understood tools.

For our study, we required an ore body with a comprehensive and publicly available information base. Profiting from recent and complete geological and geophysical information obtained at the Bathurst mining camp in New Brunswick (Thomas et al., 2000), we chose to simulate the Brunswick no. 12 deposit, which is one of the largest massive sulfide deposits in the Bathurst area. By determining synthetic AMT responses of models of the Bathurst no. 12 deposit, for different strike lengths and sampling geometries, we were able to investigate the main caveats for 2D interpretation of 3D data in a mining environment. In addition, by determining AMT responses within the earth, we examined the advantages of down-mine AMT data acquisition for resolution of below-mine ore bodies.

Although many 3D modeling studies have been published, because of the complexity of the model we studied and its closeness to geological reality, ours is a new and innovative contribution. Moreover, we present complete analyses of the model and make suggestions for a new approach, that of taking down-mine measurements.

DESIGN OF THE 3D MODEL

Figure 1 shows a geological map and cross section of the Brunswick no. 12 deposit. The design of our 3D numerical model took into account geophysical and geologic information from Thomas et al. (2000) and references therein. Following Katsube et al. (1997), zones of different resistivity, corresponding to different host rocks, were modeled. However, to emphasize our main points, we present herein only the simplest case, that of a conductive homogeneous ore body of 2 Ωm resistivity embedded in a resistive homogeneous halfspace of 1000 Ωm resistivity. To replicate local conditions, we included a thin layer of overburden (thickness 9 m) of 100 Ωm resistivity covering the ore body and the area to its east. The shape of the ore body is highly irregular, both laterally and with depth, and was interpolated from plan views of the deposit at eight different depths, obtained from Luff et al. (1992).

Figure 2 shows the 3D model ore body we constructed. Note that the ore body subcrops beneath the layer of sedimentary overburden. To allow sensitivity testing of strike length, we constructed other 3D models by varying the geometry of the initial model, particularly the X-direction length and depth to its base.

ELECTROMAGNETIC RESPONSE OF THE MODEL

The synthetic data were calculated using the 3D MT forward code of Mackie et al. (1994), with modifications from R. L. Mackie and J. R. Booker (personal communication, 1999). The 3D mesh used was a compromise between the physical parameters of the model (size of body, conductivity, depth, overburden thickness, and station locations) and computational limitations. The surface AMT synthetic responses at eleven frequencies between 10,000 and 0.04 Hz were calculated. In all cases, convergence of the response was verified by increasing the mesh size until the responses were asymptotic to stable values. The final mesh was 86 cells $(E - W) \times 99$ cells $(N - S) \times 50$ cells (vertical), with a horizontal cell size of 12.5 m within and close to the ore body. The validity of the 3D responses was also tested by comparing the 3D responses for a body of infinite length to 2D responses derived using the code of Wannamaker et al. (1987) with the same mesh size. For this mesh size, the 3D code needed 1.5 Gb of random-access memory on a Sun Blade 1000 workstation and took 48 hours to calculate responses at the eleven frequencies.

Figure 3 shows the XY (quasi-TE) and YX (quasi-TM) apparent resistivities and phases, plotted as pseudosections that would be obtained at stations located on a surface profile crossing the center of the body (see Figure 2) in the Y-(E-W) direction. Although the ore body is 3D, its elongate shape means the X-direction can be considered as the strike direction.

The most significant result was the behavior of the RhoXY apparent resistivities at low frequencies. Close to the ore body they remained anomalously low compared with those that would have been obtained for a body with infinite length (i.e., the 2D response). The phases at sites above the body were high (near 78°) but did not go beyond the first quadrant (0°–90°). It was possible to fit the XY and YX data (both apparent resistivity and phase angle) separately with two different 1D models, which implies that there is a mathematical and physical relationship between the apparent resistivities and the phases at each site and for each mode for this particular 3D model.

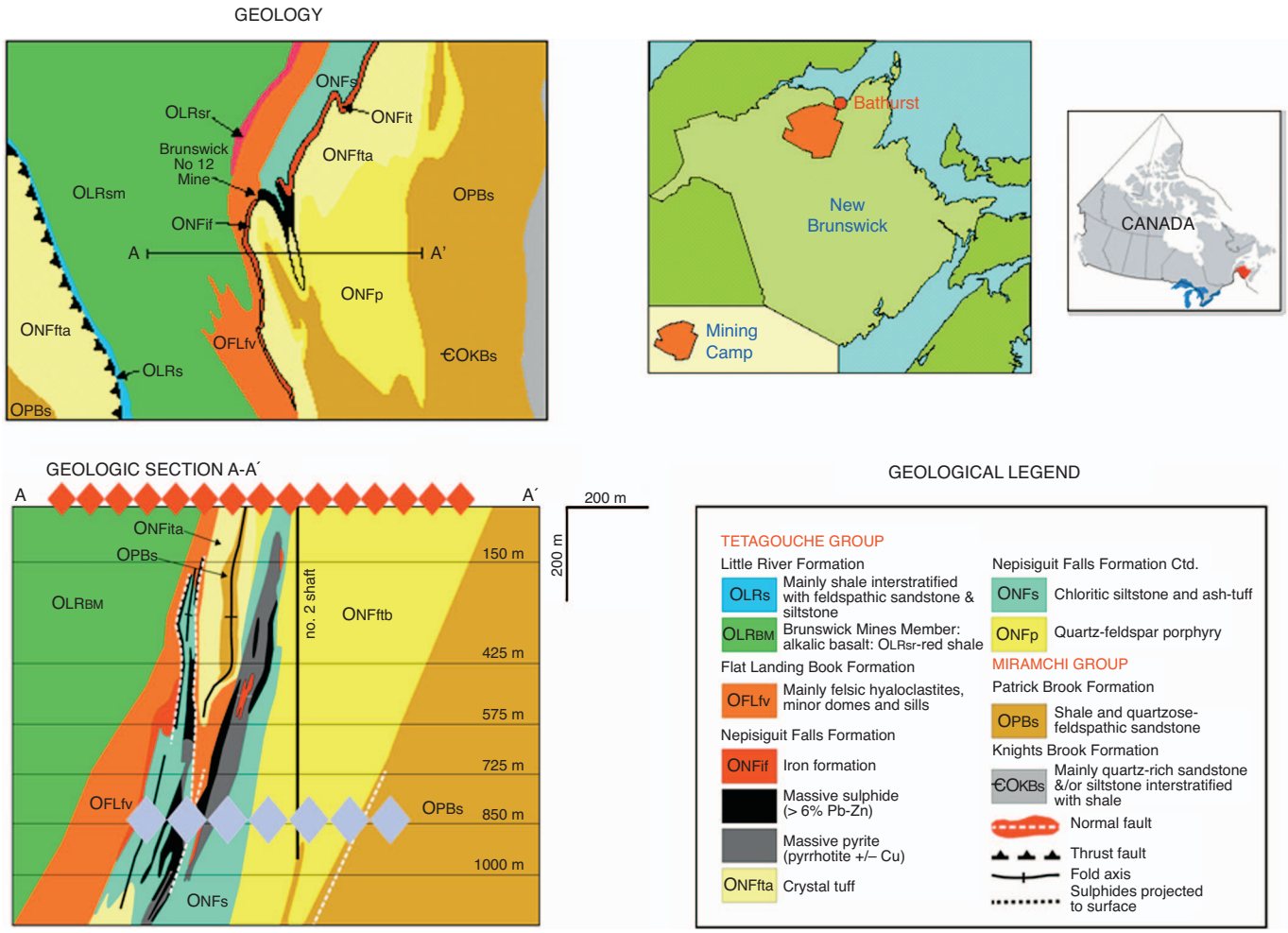

Figure 1. Geologic map and cross section of the Bathurst no. 12 deposit (from Thomas et al., 2000). The schematic locations of the surface AMT acquisition sites (red diamonds) and down-mine sites (gray diamonds) used in the modeling are also shown. The down-mine AMT sites are at the lowest level of current ore extraction.

2D INVERSION OF 3D DATA

We carried out 2D inversion tests on various subsets of the data: XY (quasi-TE) and YX (quasi-TM) data jointly, only XY or only YX, only phases or only resistivities; and using different frequency ranges and different sampling geometry. The inversions shown herein were obtained using RLM2DI code (Rodi and Mackie, 2001). We obtained similar results using other codes (RRI of Smith and Booker, 1991; and REBOCC of Siripunvaraporn and Egbert, 2000).

Table 1 summarizes the most significant of our tests, and Figure 4 presents the resultant 2D models. The YZ section beneath the profile is shown as model L of Figure 4, but it should be noted that this model is not the same as the silhouette on the Y-Z plane of Figure 2. All models presented here represent inversion of the 3D data from stations along the central profile that runs through sites 53 and 57, and the results should be compared with model L.

Model A included data from all 22 sites on the central profile. The best-fit model obtained from inversion of all data (XY as TE and YX as TM) at all 11 frequencies (model A of Figure 4) did not yield an acceptable fit; the final root mean square (rms) misfit between the synthetic 3D responses and the 2D modeled response was 4.85. (An rms misfit of unity signifies a fit within statistical tolerances with as-

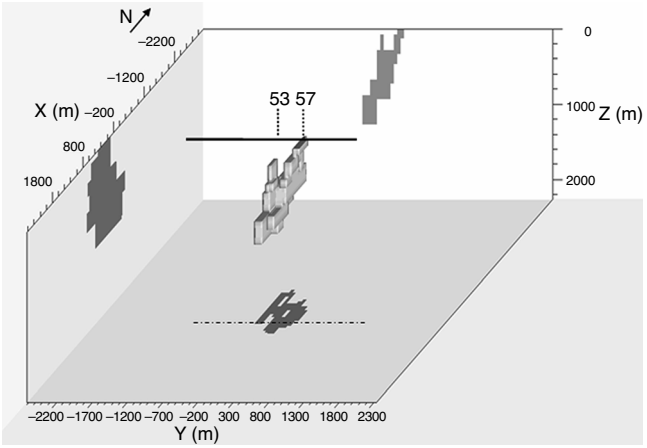

Figure 2. The numerically modeled 3D ore body used in this study (X:Y:Z is approx. 1). The profile used for 2D modeling, and the locations of recording sites 53 and 57 are also shown. The principal dimensions of the body are: depth to base, 1375 m; dip angle, 80°; maximum width in X direction (N-S), 1300 m, and in Y direction (east-west), 250 m.

sumed errors of 20% in apparent resistivity and 2.8° in-phase. These are large errors and might represent environmental and/or geologic noise.) At frequencies below 10 Hz, the XY data (quasi-TE) did not fit with a 2D model, but the YX data (quasi-TM) did. The asymptotically decreasing XY apparent resistivities at low frequencies (Figure 3) observed at sites located over the ore body were not compatible with a 2D model. When the phases alone were inverted (model B, Figure 4), the rms misfit that was achieved was statistically satisfactory (rms = 1.2), but the fit to the shape of the phase curves was poor. This suggests that some parts of the data were overfit, whereas others were underfit, which is a problem with correlated misfit residuals. The inversion of apparent resistivities and phases corresponding to the YX data (quasi-TM) alone produced a model with an acceptable final rms misfit of 1.4 (model C, Figure 4). However, although the XY data from individual sites could be fit with 1D models, there was no 2D model that fit the XY data alone; the best-fit model obtained (model D, Figure 4) had an rms misfit of 9.6.

Other inversions were performed using subsets of the higher frequency data. Using data above 10 Hz resulted in a final model with an rms misfit of 4.0 (model E). Using only the data above 100 Hz (model F) showed a good fit to the data with an rms misfit of 2.85. To study the effects on resolution of spatial sampling, other subsets were considered. Model G of Figure 4, with 16 sites, was obtained by doubling the spacing between sites used in models A to F, and models H to K had the same site geometry as model G, but the sites located directly over the body were excluded. The results show that a sample interval equal to approximately half of the body width is barely sufficient to identify the existence of the body, and is a critical limit. The rms misfit for the inversion of models H to K were satisfactory, but as the responses over the body were not inverted, the final models showed weak evidence of the body. The position and the top of the body were well resolved, in contrast to the base of the body and its resistivity which were not. To invert the lowest frequencies preferentially did not offer a solution to this inherent lack of resolution.

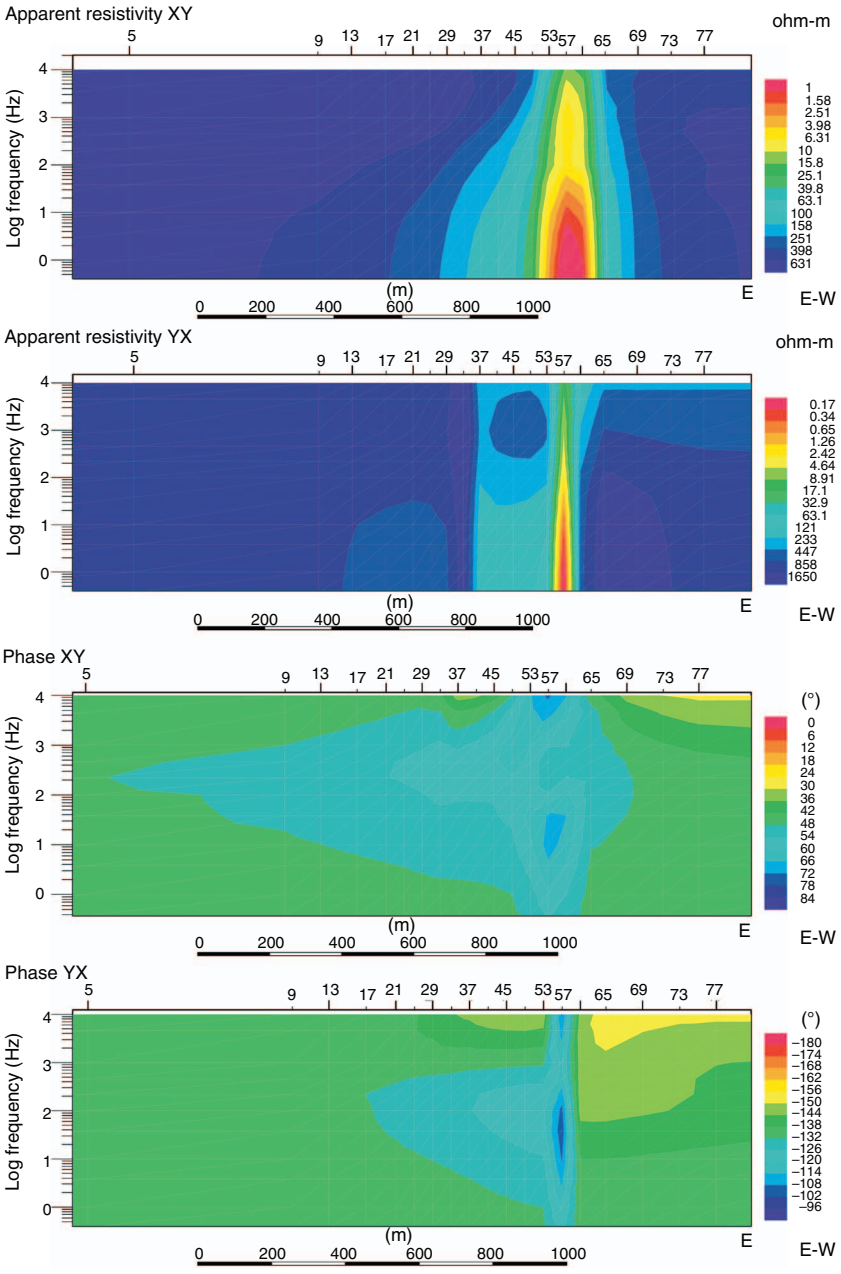

Figure 3. AMT apparent resistivities and phases for the XY (quasi-TE) and YX (quasi-TM) data along the east-west central profile crossing the ore body as shown on Figure 2.

SENSITIVITY TESTS

Figure 5 shows the apparent resistivities and phases from two sites on the central profile for effective ore body strike lengths of 500, 1000, 2500, and 10,000 m.

Site 57 was directly over the ore body and site 53 was 50 m to the west (Figure 2). At site 57, there was a sharp contrast between the responses of the XY and YX data; the XY data were sensitive to the length of strike of the body, whereas the YX data were not. This behavior held for both apparent resistivities and phases. For site 53, however, both the XY and the YX data were sensitive to strike length. At high frequencies (above 100 Hz) the behaviors of the 2D and 3D responses were similar, with phases rising to 78° at 10,000 Hz. At lower frequencies, the 3D YX data behaved as did the 2D model (rising again to 78°), but the XY data responses were completely different.

Clearly these results support the conclusions of Wannamaker et al. (1980, 1984a, b) and Jones (1983), that the quasi-TM mode responses from a 3D body can be interpreted as 2D, even for bodies of small strike length, whereas the quasi-TE model responses require long strike extents. It should be noted that for a host rock resistivity of 1000 Ωm, the skin depths at frequencies of 1000, 500, 300, and 100 Hz are 500, 700, 910, and 1580 m respectively. Conversely, the faces of the 3D body are one skin depth away for the strike ratios of 2:1 (250 m half-length), 4:1 (500 m), 10:1 (1250 m), and 40:1 (5000 m) at frequencies of 4000, 1000, 160, and 10 Hz. Figure 5 shows that

the quasi-TE responses depart from the 2D response at frequencies of 5000 Hz (2:1), 1000 Hz (4:1), 300 Hz (10:1), and 10 Hz (40:1). These values are reasonably consistent with the conclusion by Jones (1983) that the quasi-TE can be interpreted as 2D when the distance to the face of the body is more than one skin depth.

RESPONSES WITHIN THE MODEL: BELOW-MINE IMAGING

AMT measurements recorded from the lowest levels of mines can provide high-resolution below-mine imaging that might detect economic ore bodies below existing workings and thus extend mine life. We advocate two approaches: The first is to invert both the surface and down-mine AMT responses simultaneously, holding known structures constant. The second involves body stripping (a 3D version of layer stripping) by removing the responses of known 3D structures from observed down-mine responses, then treating residual responses as surface responses. Body stripping uses the fact that in 1D, MT responses at an interface depend only on the structure below that interface; that is, they are independent of any structure above it, as demonstrated by the well-known recursion relationship for deriving MT responses over layered structures (e.g., Kaufman and Keller, 1981). Body stripping gives a precise and accurate method to determine the forward response in 1D and can be a useful tool to obtain an approximation in 2D and 3D.

However, before implementing either or both of these approaches, it is important to study the nature of the forward responses within the ore body. To accomplish this, we took the 3D forward code of Mackie et al. (1994) and modified it (R. L. Mackie, personal communication, 2001) to calculate the electromagnetic fields at node points within the subsurface, and from those fields we derived apparent resistivities and phases. As stated above, the AMT impedances at any depth within a layered earth are not a function of the layers above, but for 2D and 3D models anomalous currents can flow both above and below a given depth, and thus simple stripping may be invalid.

To ascertain whether the 3D code yielded reliable numerical estimates of the EM fields within the model, we conducted several tests with layered models and compared them to 1D analytical results. Moreover, we used different meshes, refined at the locations where the fields were derived, to ensure convergence of the solutions.

After these tests, we modeled a simple 3D body of dimensions 27 m thickness, 350 m width, and 500 m length, and of 2 Ωm resistivity, hosted in a homogeneous earth of 100 Ωm resistivity. We studied the magnetotelluric responses for three cases (A-C) as described in the following section.

Case A: Body at surface versus buried

We compared the responses at the top of the body in two situations: Case A1, where the body was at the surface (z = 0 m); and case A2, where it was placed at a depth equal to its vertical thickness (i.e., with its top at z = 27 m, simulating in-mine measurement). Figure 6 shows that the apparent resistivity XY (quasi-TE) and YX (quasi-TM) pseudosections derived for both situations were very similar. The simulated measurements inside the mine (A2 in Figure 6) show that there is a conductor beneath. This behavior resembles the 1D case in that the medium above the level at which the measurements were taken has little effect. However, this is a special situation because the medium above is homogeneous and resistive, although less resistive than air. Nonetheless, this example gave us confidence in the numerical responses obtained within the earth. Note that for frequencies below 1 Hz only galvanic effects are evident.

Case B: Body at surface, measurements at different depth levels

For case B the position of the body was fixed, outcropping at the surface, and the responses were calculated for measurements at different depth levels with respect to the body: Case B1, at the top of the body (z = 0 m); case B2, at a depth corresponding to the bottom of the body (z = 27 m); and case B3, at a depth equal to twice the thickness of the body (z = 54 m). The responses for cases B1 and B2, obtained with the modified Mackie code, were compared with the 3D integral equation code of Avdeev et al. (1997) for frequencies of 10 and 100 Hz; both XY and YX apparent resistivities and phases agreed to within less than 10%. Because the degree of disagreement increased with frequency, and some numerical instabilities were observed in our solutions for 10,000 Hz, we chose to use solutions only for frequencies between 1000 and 0.1 Hz.

Figure 7 shows the apparent resistivity responses for the three variants of case B. Case B1 is the same as case A1 (Figure 6), but the responses are plotted in Figure 7 with a different color scale to facilitate comparison with cases B2 and B3. Cases B2 and B3 showed very different character to that observed in case A2 (Figure 6). The medium above the body in cases B2 and B3 had a significant influence for both polarizations, imaging a conductive zone; although, in case B3, it was smooth. Clearly, without appropriate correction, in-

Table 1. Data used for 2D inversion models of the central profile shown on Figure 2.

Model[3]	Sites and frequency band	Data inverted	Iterations	rms misfit
A	22 sites, spacing 50 m over the body All 11 frequencies (10,000–0.04 Hz)	All	66	4.85
B	As for model A	Phases only	28	1.2
C	As for model A	YX only	62	1.43
D	As for model A	XY only	19	9.56
E	Sites and spacing as for model A Frequencies above 10 Hz only	All	49	3.98
F	Sites and spacing as for model A Frequencies above 100 Hz only	All	53	2.85
G	16 sites, spacing 100 m over the body All frequencies	All	76	4.59
H	14 sites (excluding those over the body) All frequencies	All	86	3.76
I	As for model H	Phases only	9	0.99
J	As for model H	XY	29	5.64
K	As for model H	YX	67	1.09

[3]Model letters correspond to Figure 4a-k, respectively.

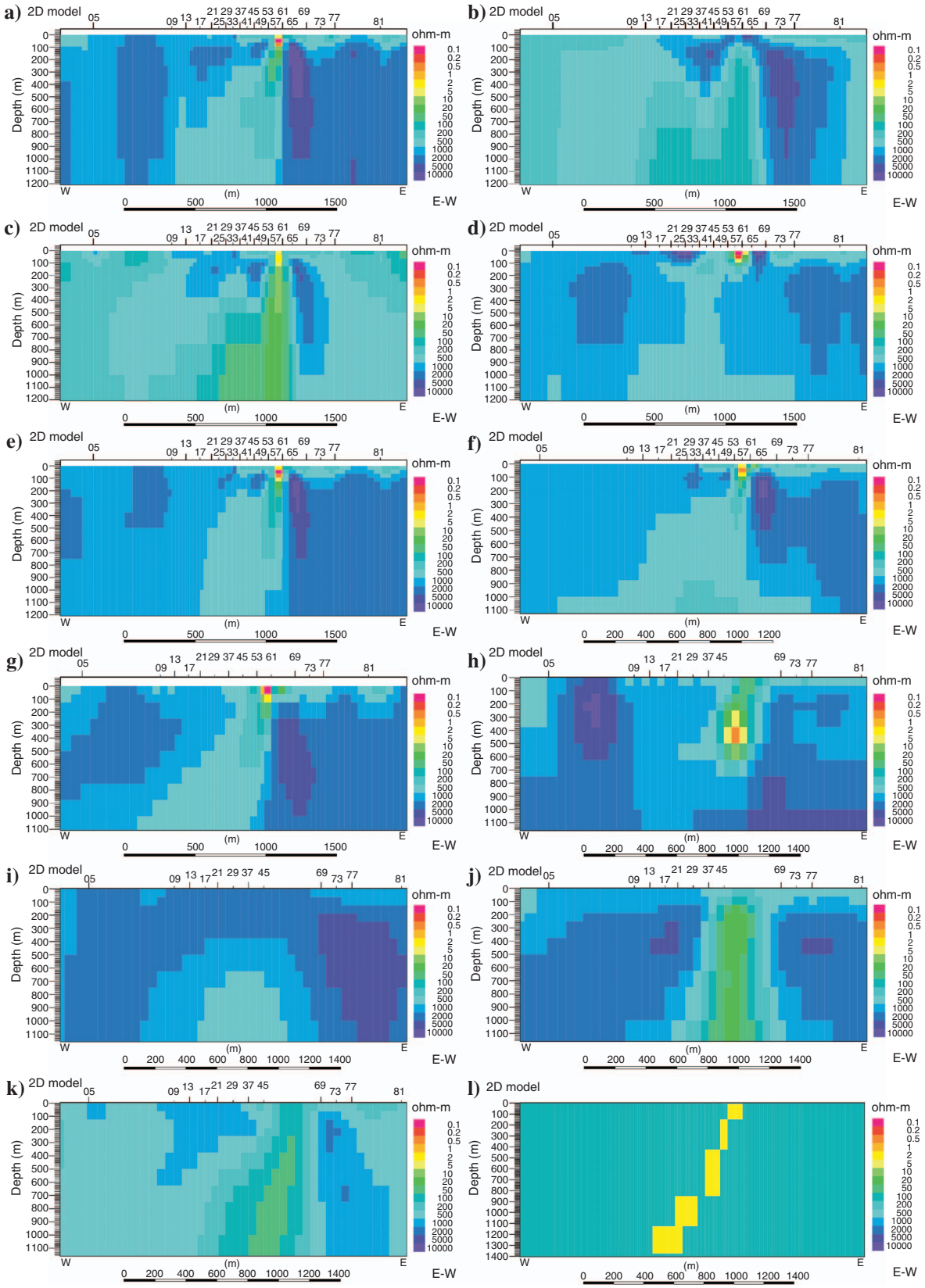

Figure 4. Key 2D models obtained from inversion of 3D data along the central profile shown on Figure 2. Table 1 provides details of the data used for each inversion. The YZ section below the central profile is shown as (l) model L.

terpretation of measurements made at either the 27 or 54 m level might lead to erroneous conclusions about the existence of structures below.

Effect of a tunnel

Because in a mine the responses inside an ore body can be obtained only from within the galleries of that mine, we considered the effect of a tunnel on apparent resistivity and phase responses. The tunnel was simulated by a prism, 2 m high, 2 m wide, and with a length of 350 m, equal to the width of the conducting body.

For case B2 (z = 27 m), we tested responses with and without a tunnel (it would be difficult to experimentally verify the latter in a mine). Figure 8 shows the apparent resistivities and phases for two sites, one within the tunnel and one away from the tunnel. Site 9 was

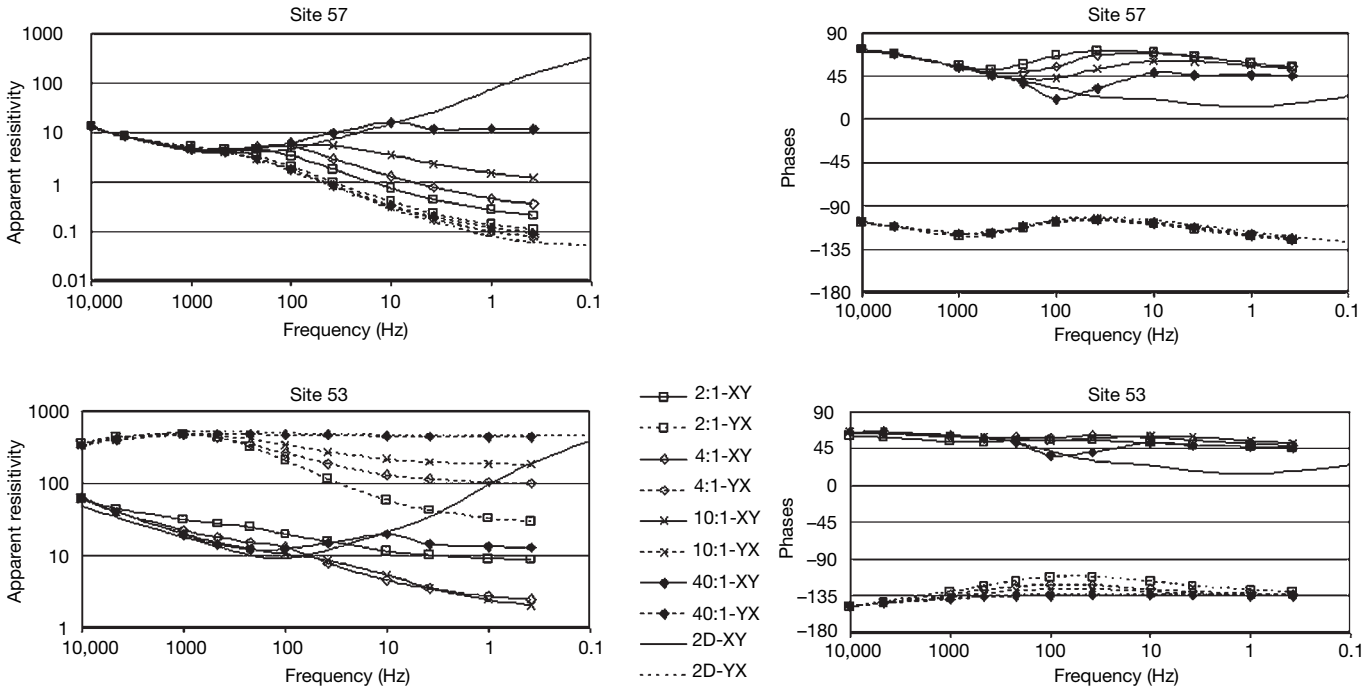

Figure 5. Comparison of the apparent resistivity and phase responses for different 3D models at two sites for varying strike length compared to the 2D response. Length to width ratios were 2:1, 4:1, 10:1, and 40:1. Site 57 was located directly over the body, and site 53 was 50 m to the west (Figure 2). The label "2D" indicates the responses calculated using the 2D forward code.

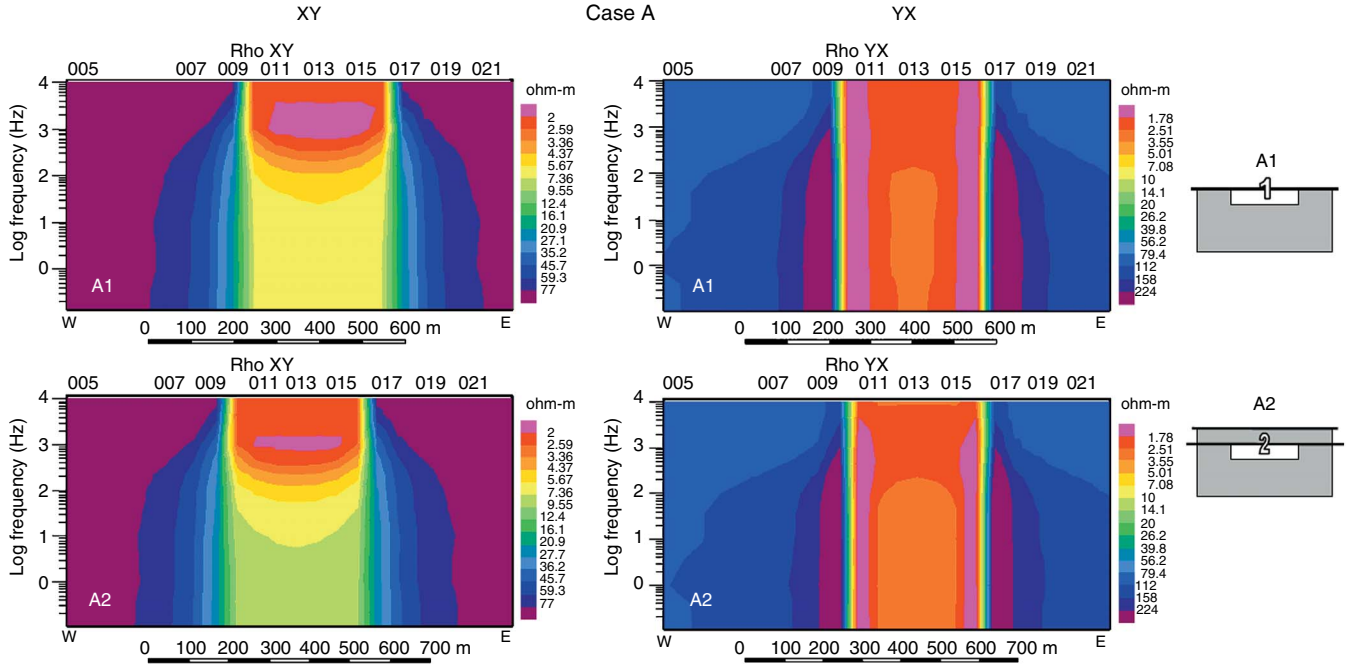

Figure 6. Apparent resistivity pseudosections (XY and YX) for: case A1, the 3D model response for a body (500 m length × 350 m width × 27 m thickness, resistivity 2 Ωm) outcropping at the surface with measurements taken at the surface, and case A2, the 3D model response for the same body buried to a depth of 27 m with measurements taken at its top surface.

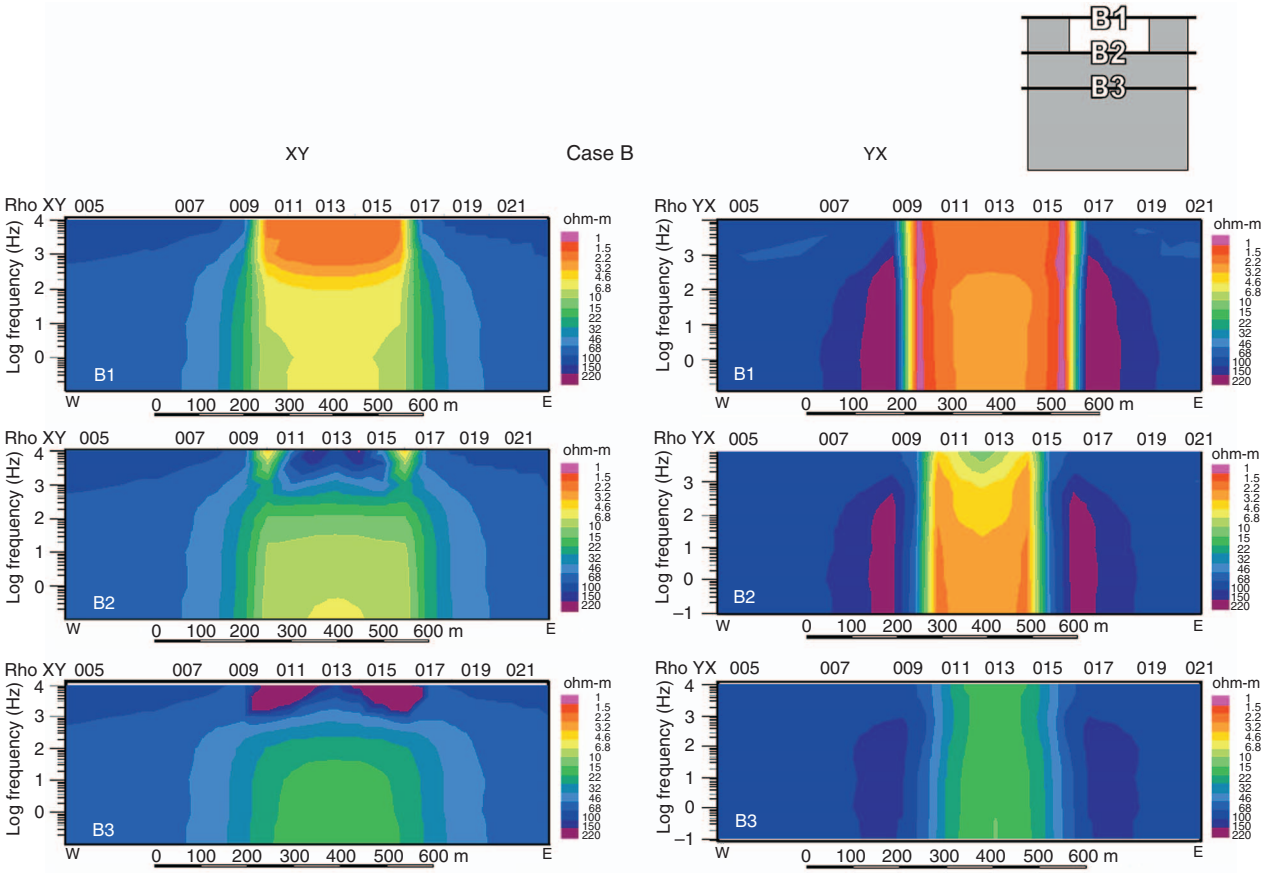

Figure 7. Apparent resistivity pseudosections for the 3D responses for a 3D body (500 m length × 350 m width × 27 m thickness, resistivity 2 Ωm). Case B1, measured at the surface (same data as case A1 of Figure 6, but with different color scale); case B2, with measurements along its basal surface at 27 m depth; and case B3, with measurements taken along a level 27 m below the base of the body (z = 54 m).

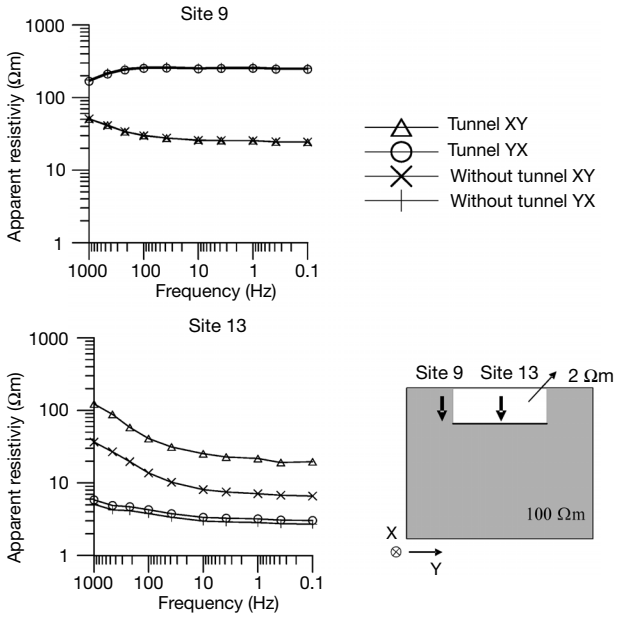

Figure 8. Simulation of the effect of a tunnel on the apparent resistivity curves for two sites. The tunnel was simulated by a body 2 m high × 2 m wide × 350 m long of 10,000 Ωm resistivity at the base of a 3D body 500 m long × 350 m wide × 27 m thick and 2 Ωm resistivity. The tunnel is shown as the dark bar at the base of body.

outside the tunnel and site 13 was inside the tunnel at the base of the conductive body. The tunnel created a distortion that can be considered as a static shift (e.g., Jones, 1988). The phases were identical with and without the effect of the tunnel, but at the site within the tunnel the apparent resistivities were shifted by a frequency-independent multiplicative constant.

To simulate the resistivity of the air within the tunnel, we tested resistivities of 5000 and 10,000 Ωm; the shift of the apparent resistivities increased with increasing resistivity of the air.

We concluded that the effect of the tunnel on apparent resistivities is important and must be taken into account for interpretations or inversions of experimental data.

Case C: Down-mine responses and body stripping

As a first approach, body stripping of the responses of known structures can be useful to reduce the effects of structures above the level of data acquisition. To examine this we derived theoretical responses as follows:

First, responses were calculated at a depth of 27 m for two 3D bodies with their top interfaces at the surface, one of 27 m thickness, and the other of 54 m thickness (cases C1 and C2, respectively). Figure 9 shows the XY apparent resistivity responses for these two cases. The difference between the two sets of responses (C2-C1) was then derived on a logarithmic scale for apparent resistivities, and on a linear scale for phases. An apparent resistivity pseudosection of the XY difference is shown in Figure 10.

Second, apparent resistivity responses were derived at a depth of 27 m for a body of 27 m thickness with its top interface at 27 m depth; that is, the responses from the top of the body, which corresponds to case A2. The resultant XY apparent resistivity pseudosection is shown in Figure 10.

Figure 11 shows the apparent resistivity curves for a site in the center of the profile on top of the body for cases C1, C2, C2–C1, body stripping, and A2. The body-stripping curve was obtained from the log-difference between the responses from cases C2 and C1, shifted upward to a resistivity of 2 Ωm at the highest frequency. The responses of the body-stripping scenario and case A2 are similar. At high frequencies, apparent resistivity increases from that of the body (2 Ωm) as frequency decreases, but the body-stripping response had a smaller galvanic distortion effect than case A2 (i.e., the response of the structure below the level of acquisition). The body stripping curve reached a maximum resistivity of 45 Ωm, whereas the curve for case A2 rose only to 8 Ωm, compared to the 100 Ωm resistivity of the surrounding medium. Thus, at lower frequencies the two diverged significantly, as can be observed by comparing the pseudosections in Figure 10.

We concluded from this simple example that body stripping may not be a successful strategy to recover accurately the response of conductive structures below the level of acquisition. However, assuming that the conductivity of the deposit and surrounding rocks can be obtained, and if the response of the overlying conductive structure is correctly stripped away, it can show qualitatively if more conductive material is present below the level of acquisition.

DOWN-MINE ELECTROMAGNETIC RESPONSE OF THE MODEL

We computed the down-mine electromagnetic responses for the ore body illustrated in Figure 2. The cross section A-A′ (Figure 1) is shown schematically in Figure 12c. The gray-shaded region represents known ore, interpolated from information from Luff et al. (1992), and the horizontal dotted line shows the lowest level of the current mine workings along which responses were computed. The apparent resistivities and phase responses from four stations, sites 17, 33, 49, and 61, are shown on Figure 12a and b. Sites 17 and 61 were neither beneath nor above ore, and their phase responses remained within their appropriate quadrants (first quadrant for XY and third quadrant for YX). In contrast, the sites that were either above ore (site 33) or below ore (site 49) exhibited phase responses that did not obey the quadrant rules for surface responses from 1D, 2D,

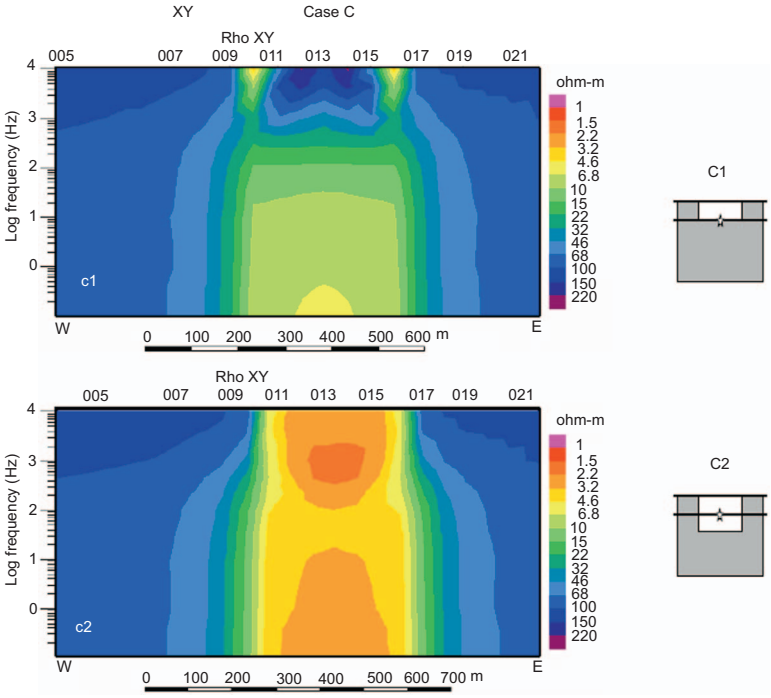

Figure 9. Apparent resistivity XY (quasi-TE) pseudosections for the 3D responses at the 27 m level within the earth for two 3D bodies. Case C1, a body 500 m long × 350 m wide × 27 m thick of 2 Ωm resistivity, measurements taken at the level of its base (same as Case B2, Figure 7 but with different color scale); case C2, a body 500 m long × 350 m wide × 54 m thick, of 2 Ωm resistivity, measurements taken at its middle level (z = 27 m).

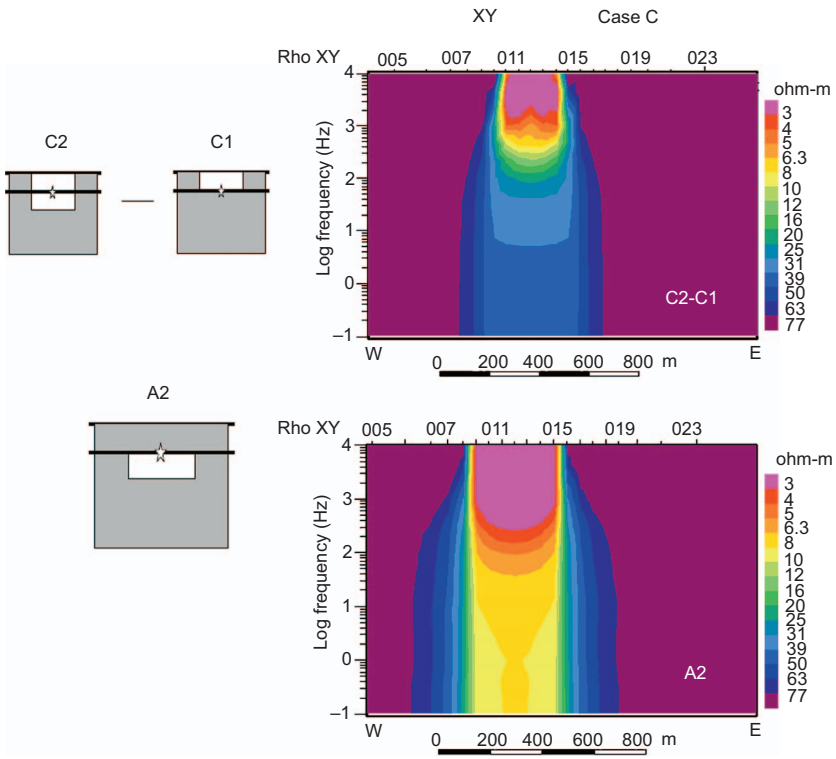

Figure 10. Comparison of apparent resistivity response (XY quasi-TE pseudosection) after body stripping (C2-C1) with response of only the structure below the level of acquisition (case A2 of Figure 6).

and 3D models, unless, of course, there is some sort of galvanic distortion (or an equivalent one) (e.g., Larsen, 1977; Richards et al., 1982; Bahr, 1988; Groom and Bailey, 1989; McNeice and Jones, 2001; Weckmann et al., 2003). The XY apparent resistivities for site 49 and the YX apparent resistivities for site 33 were also strongly distorted, with gradients exceeding one on a log-log scale. The extreme responses at sites 33 and 49 can be attributed to the complex and highly conductive structure of the ore body, which tended to gather and/or deflect horizontal electromagnetic fields and currents and, in particular, to the fact that there was conductive material both above and below the sensing location.

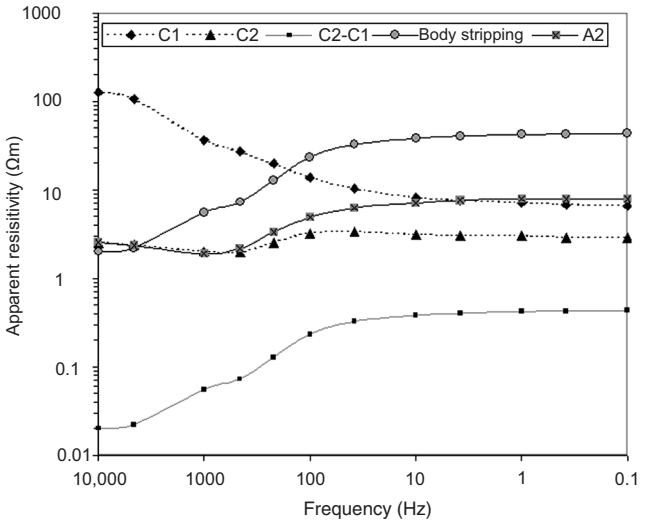

Figure 11. XY (quasi-TE) apparent resistivities observed at a site in the center of the profile at a depth of 27 Ωm for cases C1 (Figure 9), C2 (Figure 9), the difference between C2 and C1, the scaled difference between C2 and C1 (i.e., body stripping, apparent resistivity curve bulk shifted to match known body resistivity of 2 Ωm), and case A2 (Figure 6).

DISCUSSION AND RECOMMENDATIONS

From the initial results of our continuing study, we make several recommendations for the design of AMT surveys to detect and delineate ore bodies, and for interpretation of the acquired data. These recommendations are discussed below:

1) For a 3D body of limited extent, the anomalous horizontal magnetic-field components are small compared to the 2D case; most of the anomalous response is from the electric-field components. This suggests that an optimized field experiment would use stationary magnetic sensors and multiple electric-field measurements. This can be achieved with the MIMDAS (Sheard, 2001) or TITAN-24 (White and Gordon, 2003) technologies. However, in a numerical simulation of the Kidd Creek deposit, Jones and McNeice (2002) showed that if a deposit has significant length extent, the anomalies in the magnetic field can be three times greater than the anomalies in the electric field.
2) Site spacing must be sufficiently close to resolve the body; spacing of less than half the width of the body must be considered a maximum for bodies similar to the one studied here. This is especially true for MT.
3) When interpreting a 2D model, it must be kept in mind that the data corresponding to the strike-parallel electric field (XY data in this study) are more sensitive to 3D effects than the data across strike. If a 2D inversion is attempted, all the across-strike data can be considered, but only the high frequency strike-parallel data should be used. As a rule of thumb, frequencies greater than one skin depth in the host can be used in TE, and greater than one-tenth of skin depth in TM (Jones, 1983).
4) The base of an ore body is poorly resolved by the AMT method. The differences between the complete body (maximum depth 1375 in this study) and a reduced thickness body (reducing the maximum depth to 850 m) are less than 15% for the lowest frequencies.
5) The wide frequency range of AMT data is necessary to detect and to delineate the deep geometry of a 3D body, including data in the difficult AMT dead-band of Garcia and Jones (2002, 2005).

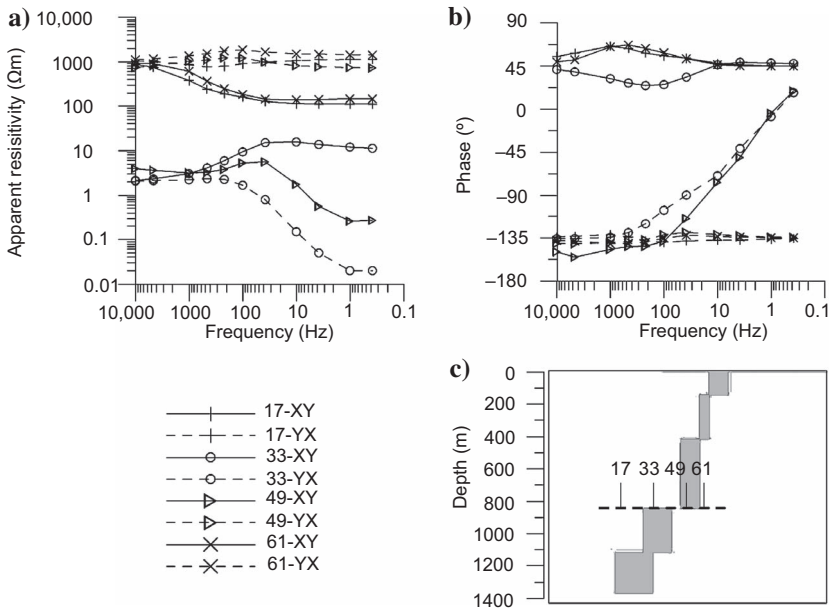

Figure 12. Down-mine electromagnetic responses of the numerical simulation model of the Bathurst no. 12 ore body at a depth of 850 m (lowest level of current ore extraction). The apparent resistivities (a) and phases (b) are those that would be observed in the XY (quasi-TE) and YX (quasi-TM) data at sites 17, 33, 49, and 61. (c) shows a sketch of the section along the profile A-A′ (Figure 1). Sites 17 and 61 are neither above nor below ore. Site 33 is above ore only, and site 49 is below ore only.

CONCLUSIONS

Tests of the ATM response to a simple model of a buried conductive body showed that conductive structures above the level from which the measurements were taken affected those measurements. These effects are important when attempting to image a conductive zone below a

known ore body. As a first approach, body stripping of the responses of known structures can be qualitatively useful to reduce these effects, but this approach cannot isolate the responses for only the deeper structures. A full inversion, fixing the known near-surface structures, must be undertaken.

Some questions about the influence of environmental and/or geological noise remain unanswered, but a useful study of the influence of noise in MT mining exploration is beyond the scope of this paper. However, our main conclusions are not dependent on the answers to these questions, which can be addressed within the framework of future studies of 3D inversion.

ACKNOWLEDGMENTS

The authors thank Randy Mackie for advice on how to modify his code to obtain responses inside the earth. They also thank Dmitry Avdeev for his help comparing some 3D responses with his code. This study was undertaken in the framework of the DIAS-UB agreement supported by Generalitat de Catalunya ACI-2003-8 and by Pla estrategic de recerca-UB 2006. The authors also thank the SEG associate editor, and referees Kevin Stevens and Phil Wannamaker for suggestions that improved this paper.

REFERENCES

Avdeev, D. B., A. V. Kuvshinov, O. V. Pankratov, and G. A. Newman, 1997, High-performance three-dimensional electromagnetic modelling using modified Neumann series: Wide-band numerical solution and examples: Journal of Geomagnetism and Geoelectricity, **49**, 1519–1539.

Bahr, K., 1988, Interpretation of the magnetotelluric impedance tensor: Regional induction and local telluric distortion: Journal of Geophysics, **62**, 119–127.

Balch, S., T. J. Crebs, A. King, and M. Verbiski, 1998, Geophysics of the Voisey's Bay Ni-Cu-Co deposits: 68th Annual International Meeting, SEG, Expanded Abstracts, 784–787.

Boerner, D. E., J. A. Wright, J. G. Thurlow, and L. E. Reed, 1993, Tensor CSAMT studies at the Buchans Mine in central Newfoundland: Geophysics, **58**, 12–19.

Caldwell, T., H. M. Bibby, and C. Brown, 2004, The magnetotelluric phase tensor: Geophysical Journal International, **158**, 457–469.

Egbert, G. D., 1997, Robust multiple-station magnetotelluric data processing: Geophysical Journal International, **130**, 475–496.

Garcia, X., and A. G. Jones, 2001, Advances in the application of audiomagnetotellurics (AMT) for mineral exploration: XXVI General Assembly, EAGE, Geophysical Research Abstracts, 3, 1458.

———, 2002, Atmospheric sources for audio-magnetotelluric (AMT) sounding: Geophysics, **67**, 448–458.

———, 2005, A new methodology for the acquisition and processing of audio-magnetotelluric (AMT) data in the AMT dead band: Geophysics, **70**, 119–126.

Garcia, X., J. Ledo, and P. Queralt, 1999, 2-D Inversion of 3-D magnetotelluric data: the Kayabe dataset: Earth, Planets and Space, **51**, 1135–1143.

Groom, R. W., and R. C. Bailey, 1989, Decomposition of magnetotelluric impedance tensors in the presence of local three dimensional galvanic distortion: Journal of Geophysical Research, **94**, 1913–1925.

Jones, A. G., 1983, The problem of "current channelling:" A critical review: Surveys in Geophysics, **6**, 79–122.

———, 1988, Static shift of magnetotelluric data and its removal in a sedimentary basin environment: Geophysics, **53**, 967–978.

Jones, A. G., A. D. Chave, D. Auld, K. Bahr, and G. Egbert, 1989. A comparison of techniques for magnetotelluric response function estimation: Journal of Geophysical Research, **94**, 14 201–14 213.

Jones, A. G., and X. Garcia, 2003, The Okak Bay MT dataset case study: A lesson in dimensionality and scale: Geophysics, **68**, 70–91.

Jones, A. G., and G. W. McNeice, 2002, Audio-magnetotellurics (AMT) for steeply-dipping mineral targets: importance of multi-component measurements at each site: 72nd Annual International Meeting, SEG, Expanded Abstracts, 21, 496–499.

Katsube, T. J., N. Scromeda, M. E. Best, and W. D. Goodfellow, 1997, Electrical characteristics of mineralized and non-mineralized rocks at the Brunswick No. 12 deposit, Bathurst mining camp, New Brunswick: Geological Survey of Canada Current Research, 97–107.

Kaufman, A. A., and G. V. Keller, 1981, The magnetotelluric sounding method: Elsevier Science Publishing Co., Inc.

Larsen, J. C., 1977, Removal of local surface conductivity effects from low frequency mantle response curves: Acta Geodaetica Geophysica et Montanistica, **12**, 183–186.

Ledo, J. J., 2005, Two-dimensional versus three-dimensional magnetotelluric data interpretation: Surveys in Geophysics, **26**, 507–669.

Ledo, J. J., P. Queralt, A. Martí, and A. G. Jones, 2002, Two dimensional interpretation of 3-D magnetotelluric data: An example of limitations and resolution: Geophysical Journal International, **150**, 127–139.

Livelybrooks, D., M. Mareschal, E. Blais, and J. T. Smith, 1996, Magnetotelluric delineation of the Trillabelle massive sulfide body in Sudbury, Ontario: Geophysics, **61**, 970–986.

Luff, W. M., W. D. Goodfellow, and S. J. Juras, 1992, Evidence for a feeder pipe and associated alteration at the Brunswick No. 12 massive-sulfide deposit: Exploration and Mining Geology, **1**, 165–185.

Mackie, R. L., J. T. Smith, and T. R. Madden, 1994, Three-dimensional electromagnetic modeling using finite differences equations: The magnetotelluric example, Radio Science, **29**, 923–935.

McNeice, G., and A. G. Jones, 2001, Multisite, multifrequency tensor decomposition of magnetotelluric data: Geophysics, **66**, 158–173.

Richards, M. L., U. Schmucker, and E. Steveling, 1982, Entzerrung der Impedanzkurven von magnetotellurischen Messungen in der Schwäbischen Alb, *in* Protokol über das 9. Kolloquium Elektromagnetische Tiefenforschung (Abstracts from 9th Electromagnetic Deep Sounding Symposium), Neustadt an der Weinstraße, Federal Republic of Germany, 22–26 March, 27–40.

Rodi, W., and R. L. Mackie, 2001, Nonlinear conjugate gradients algorithm for 2-D magnetotelluric inversion: Geophysics, **66**, 174–187.

Sheard, N., 2001, The value of advanced geophysical technology in modern exploration: Bulletin of the Australian Institute of Geoscientists, **35**, 53–56.

Siripunvaraporn, W., and G. Egbert, 2000, An efficient data-subspace inversion method for 2-D magnetotelluric data: Geophysics, **65**, 791–803.

Siripunvaraporn, W., G. Egbert, Y. Lenbury, and M. Uyeshima, 2005, Three-dimensional magnetotelluric inversion: Data-space method, Physics of the Earth and Planetary Interiors, **150**, 3–14.

Smith, J. T., and J. R. Booker, 1991, Rapid inversion of two and three-dimensional magnetotelluric data: Journal of Geophysical Research, **96**, 3905–3922.

Stevens, K. M., and G. McNeice, 1998, On the detection of Ni-Cu ore hosting structures in the Sudbury Igneous Complex using the magnetotelluric method: 68th Annual International Meeting, SEG, Expanded Abstracts, 751–755.

Stummer, P., H. R. Maurer, and A. G. Green, 2004, Experimental design: Electrical resistivity data sets that provide optimum subsurface information: Geophysics, **69**, 120–139.

Thomas, M. D., J. A. Walker, P. Keating, R. Shives, F. Kiss, and W. D. Goodfellow, 2000, Geophysical atlas of massive sulphide signatures, Bathurst Mining Camp, New Brunswick, CD-ROM version: Geological Survey of Canada Open File D3887.

Ting, S. C., and G. W. Hohmann, 1981, Integral equation modeling of three dimensional magnetotelluric response: Geophysics, **46**, 182–197.

Tripp, A. C., 2005, Acheron's rainbow: Free associations on 75 years of exploration geo-electromagnetics, Geophysics, **70**, no. 6, ND25-ND31.

Wannamaker, P. E., 1997, Tensor CSAMT survey of the Sulphur Springs thermal area, Valles Caldera, New Mexico, Parts I & II: Implications for structure of the western caldera and for CSAMT methodology: Geophysics, **62**, 451–476.

Wannamaker, P. E., G. W. Hohmann, and S. H. Ward, 1984a, Magnetotelluric responses of three-dimensional bodies in layered earths: Geophysics, **49**, 1517–1533.

Wannamaker, P. E., G. W. Hohmann, and W. A. San Filipo, 1984b, Electromagnetic modeling of three-dimensional bodies in layered earths using integral equations: Geophysics, **49**, 60–74.

Wannamaker, P. E., J. A. Stodt, and L. Rijo, 1987, A stable finite element solution for two-dimensional magnetotelluric modeling: Geophysical Journal of the Royal Astronomical Society, **88**, 277–296.

Wannamaker, P. E., S. H. Ward, G. W. Hohmann, and W. R. Sill, 1980, Magnetotelluric models of the Roosevelt Hot Springs thermal area, Utah: U. S. Department of Energy, Report: DOE/ET/27002–8.

Watts, M. D., and S. J. Balch, 2000, AEM-constrained 2D inversion of AMT data over the Voisey's Bay massive sulfide body, Labrador: 70th Annual International Meeting, SEG, Expanded Abstracts, 1119–1121.

Weckmann, U., O. Ritter, and V. Haak, 2003, A magnetotelluric study of the Damara Belt in Namibia, 2. MT phases over 90° reveal the internal structure of the Waterburg Fault/Omaruru Lineament: Physics of the Earth and Planetary Interiors, 138, 91–112.

White, M., and R. Gordon, 2003, Deep imaging: New technology lowers cost of discovery: Canadian Mining Journal, 27–28.

Zhang, P., A. King, and D. Watts, 1998, Using magnetotellurics for mineral exploration: 68th Annual International Meeting, SEG, Expanded Abstracts, 776–779.